Generation and Analysis of Interleukin-4 Deficient Mice

R. KÜHN,* K. RAJEWSKY, W. MÜLLER

Interleukin-4 (IL-4) promotes the growth and differentiation of many hematopoietic cells in vitro; in particular, it directs the immunoglobulin (Ig) class switch to IgG1 and IgE. Mice homozygous for a mutation that inactivates the IL-4 gene were generated to test the requirement for IL-4 in vivo. In the mutant mice T and B cell development was normal, but the serum levels of IgG1 and IgE were strongly reduced. The IgG1 dominance in a T cell–dependent immune response was lost, and IgE was not detectable upon nematode infection. Thus, some but not all of the in vitro properties of IL-4 are critical for the physiology of the immune system in vivo.

INTERLEUKIN-4 AFFECTS PROLIFERATION and differentiation of various cell types of the lymphoid system in vitro (*1*). B lymphocytes are induced to increase expression of major histocompatibility complex (MHC) class II molecules and the IgE low affinity receptor (CD23) (*1*); B cell proliferation in response to antibodies to Ig is enhanced (*1*). Immunoglobulin class switching of lipopolysaccharide (LPS)-activated B cells to IgG1 and IgE is directed by IL-4 in vitro (*1, 2*). Treatment of mice with antibodies to IL-4 or to the IL-4 receptor completely suppresses the production of IgE, whereas the IgG1 response to various antigens is only marginally affected (*1, 3*). The growth promoting activities of IL-4 on fetal thymocytes and mature T cells suggest a possible function in T cell development (*1, 4*). In addition, this cytokine influences the growth, differentiation, or both, of mast cells, macrophages, and hemopoetic progenitor cells (*1, 5*). A helper T cell population (T_H2 cells) (*6*) and mast cells (*5*) produce IL-4. The multiple in vitro effects suggest that IL-4 is important in T cell–dependent immune responses and that its action is pleiotropic.

To reveal the essential functions of IL-4 in vivo, without the possible limitation of incomplete and time-restricted inactivation of IL-4 with the use of neutralizing antibodies, we generated an IL-4–deficient mouse mutant by gene-targeting in murine embryonic stem (ES) cells (7). The vector used for the disruption of the IL-4 gene contained a genomic fragment spanning exons 1 and 2. The *IL4T* mutation was created by the insertion of a translational stop codon and a neomycin resistance gene (*neo*^{r}) into the first exon. At the 3′ end of the genomic sequence we placed the herpes simplex virus thymidine kinase gene (*HSVtk*) to permit selection against random integration (Fig. 1A) (*8*).

The linearized vector was introduced by electroporation into ES cells and resistant colonies were selected with G418 and Gancyclovir (GANC) (*8*). The ES cell clones carrying the *IL4T* mutation on one allele through a homologous recombination event were identified by polymerase chain reaction (PCR), and the structure of the targeted locus was verified by Southern (DNA) blot analysis (Fig. 1B). Cells of two independent mutant clones were injected into blastocysts of C57BL/6 mice and the resulting male chimeras were mated to C57BL/6 females to test for germ line transmission of the *IL4T* mutation. Offspring derived from ES cells were identified by coat color and tested for the presence of the *IL4T* allele by Southern blotting (Fig. 1B). By interbreeding heterozygous offspring we obtained homozygous mutant animals that were, due to the breeding strategy, on the (129/Ola × C57BL/6)F_2 hybrid background. Two independent homozygous mutant strains, IL4T1 and IL4T9, showed the same phenotype in all experiments performed.

In order to verify that the *IL4T* mutation abrogated function, we analyzed lymphokine production in supernatants of cultured concanavalin A (Con A)–stimulated spleen cells from IL4T and control mice. The animals had been infected 8 days before with the nematode *Nippostrongylus brasiliensis* (Nb), which leads to the enhanced production of IL-4 in such cultures (*9*). IL-4 activity, measured by the ability of IL-4 to increase MHC class II expression on B cells, was at least 800 times higher in culture supernatants derived from littermate controls than in supernatants from IL4T mice, which contained no detectable IL-4 activity (Fig. 2). MHC class II induction in cultures from control mice was completely blocked by the addition of antibody to IL-4 and was also detected in the presence of a constant amount of supernatant derived from homozygous mutant mice, excluding the possibility that IL-4 was masked in the latter cultures by an inhibitor (Fig. 2). We detected in all supernatants similar amounts of interferon-γ and interleukin-2 (*10*), which indicates that mitogen stimulation was equally effective in all cultures. Because the mutant mice produced at most 1/800 of the IL-4 of control animals, we conclude that the *IL4T* mutation inactivates the IL-4 gene functionally, although we cannot formally exclude the production of an IL-4–like activity below that amount from the 3′ part of the *IL4T* allele.

IL-4 and IL-4 receptors are expressed in fetal thymus, and IL-4 acts in vitro as a T cell growth factor (*1, 4*); thus, an IL-4 deficiency may cause profound alterations in T cell development. We analyzed the T cell compartment in thymus, spleen, and lymph

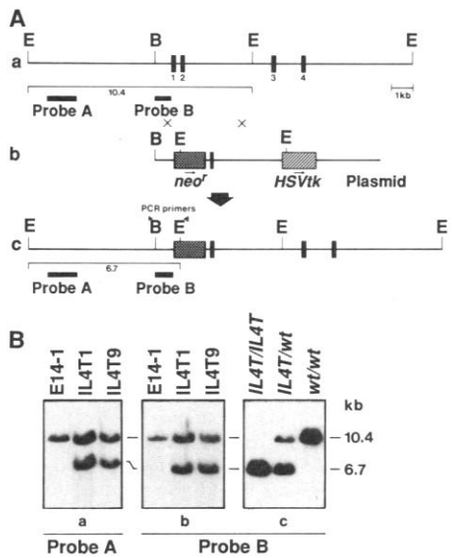

Fig. 1. (**A**) Strategy for the disruption of the IL-4 gene. (a) Genomic structure of the IL-4 wild-type locus. Exons are represented by black bars. The lengths of diagnostic restriction fragments and location of probes used for Southern blot analysis are shown. E, Eco RI; B, Bam HI. (b) Targeting vector that contains a 4.5-kb Bam HI–Eco RI fragment, which includes the first two exons of the IL-4 gene (*16, 17*). The vector was introduced by electroporation into ES cells (*18*). (c) Predicted structure of the targeted IL-4 locus. (**B**) Southern blot analysis of PCR-positive transfectants and the progeny of germ line chimeras. (a) Eco RI–digested genomic DNAs of two transfectants (IL4T1 and IL4T9) and the parental cell line (E14-1) were hybridized to probe A. The transfectants had a 6.7-kb fragment derived from the targeted IL-4 locus in addition to the 10.4-kb wild-type fragment. (b) Probe B, hybridizing only to the same 6.7-kb fragment, proves the presence of one copy of the (disrupted) IL-4 gene in the modified locus (*19*). (c) Probe B was hybridized to Eco RI–digested tail DNA from offspring of heterozygous mutant animals, obtained from germ line chimaeras generated with the IL4T1 ES cell clone. Homozygous mutant mice (*IL4T/IL4T*) show only the 6.7-kb fragment of the mutant allele, whereas heterozygotes (*IL4T/wt*) show in addition the 10.4-kb band from the wild-type (*wt/wt*) allele.

Institute for Genetics, University of Cologne, W-5000 Cologne 41, Germany.

*To whom correspondence should be addressed.

nodes of IL4T and littermate control mice by flow cytometry. No obvious difference in absolute cell numbers or the proportion of T cell subsets as defined by the CD4 and CD8 markers was observed, except that 6-week-old mutant mice had twice the thymocytes than the controls (Table 1). The B cell compartment in IL4T mice, with respect to pre-B and B cell numbers in bone marrow, spleen, and lymph nodes, and to the number of peritoneal $CD5^+$ B cells, is normal (*11*).

Analysis of antibody isotypes in the serum of 6-week-old IL4T mice showed that IgG1 was about one-sixth that of control mice (*12*), but IgM, IgG2b, IgG2a, and IgA isotypes were normal (Fig. 3). Immunoglobulin E was undetectable in the sera of five of six IL4T mice (<0.015 μg/ml) (*13*), whereas the control group IgE concentration ranged around 0.1 μg/ml (Fig. 4, day 0). Infection with Nb (*1, 3, 9, 14*) increased the serum IgE of normal animals to 5 to 50 μg/ml by day 12. In contrast, the IgE levels of all homozygous mutants remained below the detection limit (<0.015 μg/ml) (Fig. 4, day 12). Therefore, IL-4 is essential for the induction of an IgE response in vivo, and this result confirms earlier observations from in vivo studies that used IL-4 neutralizing antibodies (*3*).

We tested whether mutant mice would mount an IgG1 response upon immunization with (4-hydroxy-3-nitrophenyl)acetyl (NP)–chicken γ-globulin (CG). The CG-binding antibodies were measured at day 14 of the response and their relative concentrations were quantified in relation to NP-binding standard antibodies of the various isotypes (Fig. 5). In comparison to the controls, mutant mice had one-third to one-half the CG-specific IgG1, but IgG2b and IgG2a were increased 10 to 20 times, and IgG3 was increased about three times. The overall extent of the response, determined by the concentration of κ- and λ-bearing antibodies to CG, was similar in both groups of mice, indicating that T helper function per se was not affected. Plotting the contribution of the various isotypes to the response of each individual mouse revealed that the dominance of IgG1, as seen in normal animals (>95% IgG1), is lost in the homozygous mutants (40 to 50% IgG1) (Fig. 5B). Instead, 50 to 60% of the response of the latter consists of other Ig classes, mainly IgG2a and IgG2b. The isotype distribution of the antibody response to NP was similar (*15*). Thus, IL-4 appears to be responsible for the dominance of IgG1 in a T cell–dependent immune response, but is not essential for its production.

Taken together, our results establish an important role of IL-4 in Ig isotype selection in vivo, in accord with earlier data obtained through the use of antibodies to IL-4 and the IL-4 receptor (*3*) and the analysis of isotype switching in vitro (*2*). However, IL-4 is not essential for the mouse, and, in the limits of the present study, B and T cell development proceeds normally in its absence, except for the expression of IgG1 and IgE antibodies. It remains to be seen whether other, more intricate, features of lymphocyte differentiation are undisturbed in mice carrying the *IL4T* mutation, such as the possible differentiation of T helper cells into the T_H1 and T_H2 subsets (*6*). Interleukin-4 is a growth factor for murine T_H2 cells in vitro, and a block of T_H2 differentiation would by itself affect antibody isotype selection (*6*).

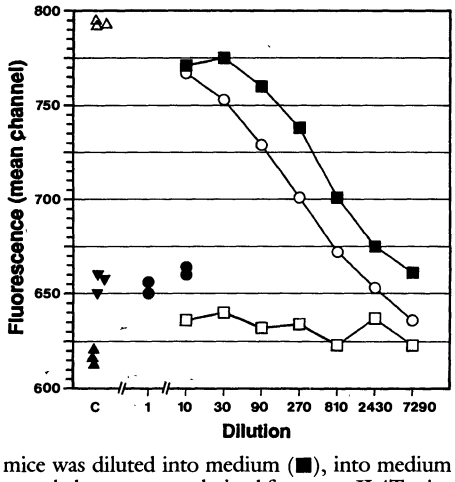

Fig. 2. IL-4 activity in Con A–stimulated spleen cell cultures of Nb-infected IL4T and littermate control mice. Spleen cells (3×10^6/ml) of mice subcutaneously infected 8 days before with 500 third-stage Nb larvae were stimulated for 20 hours with Con A (3.5 μg/ml) in CG-medium (trademark of Camon, Wiesbaden, Germany) with 5% FCS. Supernatants were tested for IL-4 activity by their ability to increase MHC class II expression on splenic B cells from normal mice. Spleen cells (10^4) were cultured for 18 hours in CG-medium (100 μl) containing 5% FCS plus supernatant (100 μl) diluted as indicated. Cells were harvested, stained with fluorescein isothiocyanate (FITC)–coupled monoclonal antibody (MAb) to I-A M5/114 (*20*) and 2500 cells were analyzed on a FACScan (Becton Dickinson). The mean channel fluorescence of the I-A–positive cells was calculated using FACscan research software. Pooled supernatant derived from two control mice was diluted into medium (■), into medium with MAb to IL-4 (11B11; 2 μg/ml) (*19*) (□), or into pooled supernatant derived from two IL4T mice (○). Supernatants derived from two IL4T mice were diluted into medium (●). c, controls: medium control (▼), in the presence of MAb to IL-4 (▲), or in the presence of an excess of recombinant IL-4 (△) (*21*).

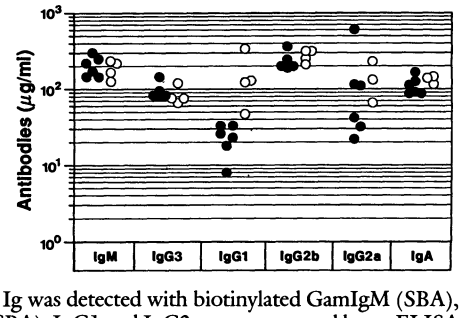

Fig. 3. Serum concentrations of Ig isotypes in IL4T and littermate control mice. Six-week-old IL4T (●) and control mice (○) were bled from the tail vein and the serum concentrations of the indicated isotypes were determined by an enzyme-linked immunosorbent assay (ELISA) (*22*). Plastic plates were coated with MAb R33-24-12 (*20*) for the detection of IgM, with goat antibody to mouse (Gam) IgG3 [Southern Biotechnology Associates, Birmingham, Alabama (SBA)] for IgG3, with MAb R14-50 (*20*) for IgG2b and with MAb 11-44-2-23-2 (*20*) for the detection of IgA. Diluted serum samples were added and bound Ig was detected with biotinylated GamIgM (SBA), GamIgG3 (SBA), GamIgG2b (SBA), or GamIgA (SBA). IgG1 and IgG2a were measured by an ELISA inhibition assay in the presence of 0.05% Tween 20. Plates were coated with IgG1 or IgG2a MAb and a 1:1 mixture of diluted serum samples and biotinylated GamIgG1 (SBA) or GamIgG2a (SBA), at a concentration tested for maximal sensitivity, was added. Serum Ig concentrations were calculated using MAbs of the various isotypes as standards. Each symbol represents the value obtained from one animal.

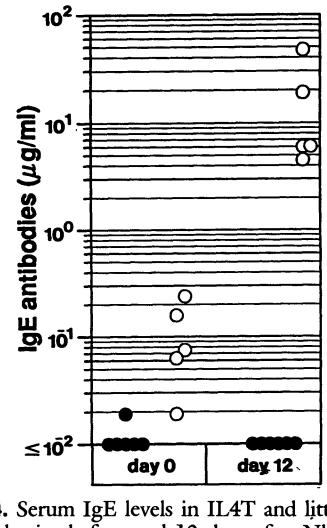

Fig. 4. Serum IgE levels in IL4T and littermate control mice before and 12 days after Nb infection. Six-week-old IL4T (●) and control (○) mice were subcutaneously infected with 500 third-stage Nb larvae, and the serum IgE levels before (day 0) and 12 days after infection were determined by an ELISA (*22*) in the presence of 0.05% Tween 20. Plastic plates were coated with rabbit antibody to mouse IgE (MIAB, Uppsala, Sweden), diluted serum samples were added, and bound IgE was detected with the MAb 95.3 (*20*). Serum IgE concentrations were calculated using a monoclonal IgE antibody as the standard. Each symbol represents the value obtained from one animal.

Table 1. Analysis of the T cell compartment in IL4T and control mice. Single-cell suspensions were prepared from thymus, spleen, and mesenteric lymph nodes of individual mice. The cell numbers were determined in a hemocytometer. Cells were stained first with biotinylated anti-CD4 (MAb GK1.5) (*20*) and in the second step with FITC-coupled anti-CD8 (MAb 53-6.72) (*20*) plus streptavidin-phycoerythrin. Dead cells were excluded from the analysis by the addition of propidium iodide. The flow cytometric analysis was performed on a FACScan with FACScan Research Software.

Mouse strain	Age (weeks)	Thymus				Spleen			Lymph node		
		Cell number	Percent			Cell number	Percent		Cell number	Percent	
			$CD4^+8^+$	$CD4^+8^-$	$CD4^-8^+$		$CD4^+8^-$	$CD4^-8^+$		$CD4^+8^-$	$CD4^-8^+$
IL4T1	4	6.5×10^7	83	13	3	3.2×10^7	11	3	2.8×10^6	53	20
IL4T9	4	5.0×10^7	87	10	2	2.8×10^7	14	4	4.0×10^6	46	18
WT1	4	6.0×10^7	83	13	3	3.0×10^7	12	3	3.2×10^6	53	23
WT9	4	6.5×10^7	87	10	2	2.4×10^7	12	4	3.4×10^6	50	17
IL4T1	6	7.0×10^7	74	18	4	3.5×10^7	13	6	3.6×10^6	46	21
IL4T9	6	7.0×10^7	74	17	4	3.0×10^7	17	9	5.2×10^6	44	23
WT1	6	3.3×10^7	70	20	7	3.6×10^7	17	9	6.4×10^6	38	27
WT9	6	3.2×10^7	77	17	4	3.0×10^7	17	7	6.4×10^6	45	22

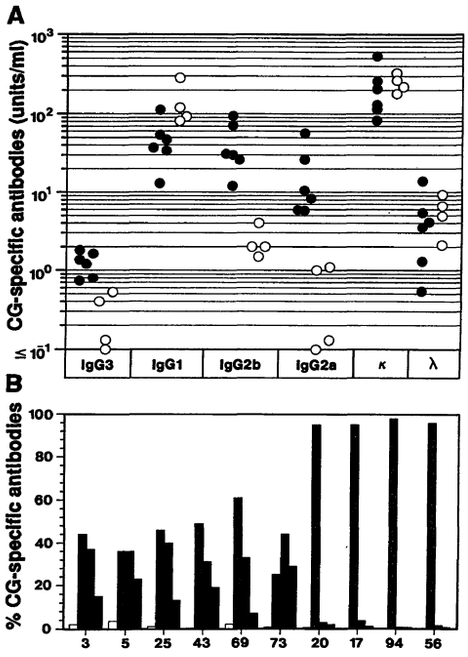

Fig. 5. Serum concentrations and isotype distribution of CG-binding antibodies in IL4T and littermate control mice after immunization with NP-CG. (**A**) Six-week-old IL4T (●) and control (○) mice were injected intraperitoneally with alum-precipitated NP-CG (100 μg per mouse) and sera were collected 14 days later. The relative serum concentrations (units/ml) of CG-binding antibodies of the indicated isotypes were determined by an ELISA (*23*). Each symbol represents the value obtained from one animal. (**B**) The values of the various isotypes of the anti-CG response of each individual animal were added, and their relative contributions (%) to the sum are shown. IL4T mice: numbers 3, 5, 25, 43, 69, and 73; control animals: numbers 20, 17, 94, and 56. Order of columns: IgG3, IgG1, IgG2b, and IgG2a.

REFERENCES AND NOTES

1. W. E. Paul and J. Ohara, *Annu. Rev. Immunol.* **5**, 429 (1987); F. D. Finkelman *et al.*, *ibid.* **8**, 303 (1990).
2. P. C. Isakson, E. Pure, E. S. Vitetta, P. H. Krammer, *J. Exp. Med.* **155**, 734 (1982); P. Sideras, S. Bergstedt-Lindqvist, E. Severinson, *Eur. J. Immunol.* **15**, 593 (1985); R. L. Coffman *et al.*, *J. Immunol.* **136**, 4538 (1986); A. Radbruch, W. Müller, K. Rajewsky, *Proc. Natl. Acad. Sci. U.S.A.* **83**, 3954 (1986); Rothman *et al.*, *J. Exp. Med.* **168**, 2385 (1988); C. Esser and A. Radbruch, *EMBO J.* **8**, 483 (1989); H. Illges, W. Müller, A. Radbruch, in *Molecular Biology of B Cell Development*, vol. 3 of *Cytokines*, C. Sorg, Ed. (Karger, Basel, 1990), pp. 109–125.
3. F. D. Finkelman *et al.*, *Proc. Acad. Sci. U.S.A.* **83**, 9675 (1986); F. D. Finkelman *et al.*, *Int. Immunol.* **3**, 599 (1991).
4. S. R. Carding, A. C. Hayday, K. Bottomly, *Immunol. Today* **12**, 239 (1991).
5. M. A. Brown *et al.*, *Cell* **50**, 809 (1987); D. Rennick *et al.*, *Proc. Natl. Acad. Sci. U.S.A.* **84**, 6889 (1987); A. Zlotnik, M: Fischer, N. Roehm, D. Zipori, *J. Immunol.* **138**, 4275 (1987).
6. T. R. Mosmann and R. L. Coffman, *Annu. Rev. Immunol.* **7**, 145 (1989). T. R. Mosmann and K. W. Moore, *Immunol. Today* **12**, A49 (1991).
7. M. R. Capecchi, *Science* **244**, 1288 (1989).
8. S. L. Mansour, K. R. Thomas, M. R. Capecchi, *Nature* **336**, 348 (1988).
9. F. J. Savelkoul, B. W. P. Seymour, L. Sullivan, R. L. Coffman, *J. Immunol.* **146**, 1801 (1991).
10. Interferon-γ was detected by an ELISA and interleukin-2 by T cell proliferation in the presence of the MAb to IL-4 11B11 (*19*); R. Kühn and W. Müller, unpublished results.
11. The B cell compartment was analyzed as described [W. Müller *et al.*, *Eur. J. Immunol.* **19**, 923 (1989)]; CD23 expression was low on splenic B cells from 4/4 IL4T mice compared to 1/4 control mice; R. Kühn and W. Müller, unpublished results.
12. The IgG1 concentrations shown in Fig. 3 were 21 ± 9 μg/ml for IL4T and 126 ± 109 μg/ml for control mice. Analyzing the IgG1 serum titer of an independent group of IL4T mice we observed a 93% decrease at the age of 6 weeks (IL4T mice, 55 ± 35 μg/ml; control mice, 739 ± 236 μg/ml) and a 98% decrease at the age of 11 weeks (IL4T mice, 44 ± 17 μg/ml; control mice, 1938 ± 222 μg/ml) in IL4T compared to littermate control mice.
13. The serum concentration of IgE in one IL4T mouse was 0.02 μg/ml before Nb infection, but was below 0.015 μg/ml after infection. We found so far that 2/15 sera from IL4T mice had IgE concentrations just above our detection limit. Given the complexity of serology and the low frequency of positive sera, we are not sure that they are real.
14. P. Lebrun and H. L. Spiegelberg, *J. Immunol.* **139**, 1459 (1987).
15. R. Kühn and W. Müller, unpublished results.
16. Phage clones spanning the IL-4 gene were isolated from a genomic library using an IL-4 cDNA probe. Eco RI fragments were subcloned into plasmid vectors and partially sequenced. The sequences were found to be identical to that described by T. Otsuka *et al.*, *Nucleic Acids Res.* **15**, 333 (1987).
17. Codon 16 of the IL-4 gene was changed to TAG followed by a newly inserted Sal I site by site-directed mutagenesis. The fragment was inserted into the Xho I site of pic19R/MC1-TK (8) and an Xho I–Sal I fragment (neo^r) of pMC1neo-polyA [K. R. Thomas and M. R. Capecchi, *Cell* **51**, 503 (1987)] was ligated into the newly created Sal I site. The pMC1neo-polyA plasmid used did not contain the point mutation described by R. L. Yenofsky, M. Fine, J. W. Pellow, *Proc. Natl. Acad. Sci. U.S.A.* **87**, 3455 (1990).
18. E14-1 cells, a subclone of the ES cell line E14 [M. Hooper, K. Hardy, A. Handyside, S. Hunter, M. Monk, *Nature* **326**, 292 (1987)] were transfected with 25 μg/ml of the linearized vector as described (*8*). ES cells were cultured in DMEM with 15% FCS, 0.1 mM 2-mercaptoethanol, 1 mM Na-pyruvate, and a saturating amount of myeloid leukemia inhibitory factor (LIF) [R. L. Williams *et al.*, *Nature* **336**, 685 (1988)]. After electroporation the cells were subjected to double selection with G418 and GANC (*8*). Surviving colonies were screened for the correct homologous recombination event by PCR analysis [D. Kitamura, J. Roes, R. Kühn, K. Rajewsky, *Nature* **350**, 423 (1991)] with the primers indicated in Fig. 1A, c. The frequency of PCR-positive clones was 1/8 resistant colonies.
19. The structure of the targeted locus was confirmed using additional probes and enzymatic digestions; R. Kühn, unpublished results.
20. MAbs used: M5/114 [A. Bhattacharya, M. Dorf, T. A. Springer, *J. Immunol.* **127**, 2488 (1981)], 11B11 [J. Ohara and W. E. Paul, *Nature* **315**, 333 (1985)], GK1.5 [D. P. Dialynas *et al.*, *J. Immunol.* **131**, 2445 (1983)], 53-6.72 [I. A. Ledbetter and L. A. Herzenberg, *Immunol. Rev.* **47**, 63 (1979)], R33-24-12 [R. Grützmann, thesis, University of Cologne (1981)], R14-50 [C. Müller, thesis, University of Cologne (1983)], 11-44-2-23-2 [J. F. Kearney, unpublished], 95.3 [M. Baniyash and Z. Eshbar, *Eur. J. Immunol.* **14**, 799 (1984)], Ig(1a)8.3 [V. T. Oi and L. A. Herzenberg, *Mol. Immunol.* **16**, 1005, (1979)], G12-47/30 [G. Seemann, thesis, University of Cologne (1981)], R33-18-10-1 [R. Grützmann, thesis, University of Cologne (1981)], Ls136 [M. Reth, thesis, University of Cologne (1981)].
21. IL-4 was also undetectable in the supernatants derived from Con A–activated spleen cells of IL4T mice in an IL-4 specific ELISA (at least 94% less, compared to control supernatants) and in a proliferation assay using an IL-4–dependent T cell clone (at least 98% less, compared to control supernatants); R. Kühn and W. Müller, unpublished results.
22. C. Kendall, I. Ionescu-Matiu, G. R. Dreesman, *J. Immunol. Meth.* **56**, 319 (1984).
23. Plastic plates were coated with CG (10 μg/ml). Diluted serum samples were added, and bound Ig was detected with biotinylated goat antibody to mouse (Gam) IgG1 (SBA), further absorbed on Sepharose coupled to IgG3, IgG2a, and IgG2b, for the determination of IgG1, with GamIgG3 (SBA) for IgG3, with MAb Ig(1a)8.3 (*20*) for $IgG2a^a$, with MAb G12-47/30 (*20*) for $IgG2a^b$, with MAb R14-50 (*20*) for IgG2b, with MAb R33-18-10-1 (*20*) for κ and with MAb Ls136 (*20*) for the detection of λ1-bearing antibodies to CG. The

relative concentration of isotypes was determined in comparison to monoclonal NP-binding standard antibodies of the same isotypes measured on a NIP_{15}-BSA coat (10 μg/ml), except for IgG2a^a. IgG2a^a was indirectly quantified in comparison to a serum of an (IgH^a × IgH^b)F_1 mouse assuming that CG-binding antibodies of both IgG2a allotypes have the same concentration. The amounts of κ- and λ1-bearing antibodies to CG were determined in relation to a κ- or λ1-bearing anti-NP standard. Assuming that the affinities of the anti-CG antibodies and the NP-binding standards are not widely different from each other, 1 unit of antibody to CG corresponds roughly to 1 μg. The procedure to determine anti-CG concentrations via anti-NP standards seems reasonable as the sum of the anti-CG isotypes were close to 50% of the sum of the κ and λ antibodies to CG in all cases. The titers for IgM and IgA were close to the limit of detection and are therefore not included in the figure.

24. We thank R. Dildrop, C. Esser, and A. Radbruch for reading the manuscript, R. Devos for the IL-4 cDNA clone, T. Blankenstein for the help during the isolation of the IL-4 genomic clone, R. Coffmann for lymphokine ELISA reagents, E. Schmitt for lymphokine ELISA reagents and for performing the T cell proliferation assay, Mr. Haider for nematode larvae, Genetics Institute for a LIF-producing cell line, M. Hooper for E14 ES cells, B. Hampel, C. Hachenberg, and C. Göttlinger for technical assistance, and U. Ringeisen for the preparation of the figures. The animal work was in accordance with official regulations. Supported by the Bundesministerium für Forschung and Technologie through the Genzentrum Köln, the Land Nordrhein-Westfalen, and the Fazit Foundation.

3 September 1991; accepted 7 October 1991

An Inducible Bundle-Forming Pilus of Enteropathogenic *Escherichia coli*

JORGE A. GIRÓN,*† ALICE SUK YUE HO, GARY K. SCHOOLNIK†

Enteropathogenic *Escherichia coli* (EPEC), a cause of childhood diarrhea, grow on the surface of the small intestine and on cultured epithelial cells as colonies of adherent bacteria. When propagated on solid medium containing blood or attached to HEp-2 cells, EPEC express ropelike bundles of filaments, termed bundle-forming pili (BFP), that create a network of fibers that bind together the individual organisms. BFP were found to be expressed by five EPEC serogroups, each harboring a ~92-kilobase plasmid previously known to be important for virulence in humans. When two of these strains were cured of this plasmid, they neither expressed BFP nor grew as adherent colonies. An antiserum to BFP reduced the capacity of EPEC to infect cultured epithelial cells. BFP are composed of a repeating subunit of 19,500 daltons, the amino-terminal amino acid sequence of this subunit is homologous to that of the toxin-coregulated pilin of *Vibrio cholerae*.

BACTERIAL PATHOGENS THAT INFECT mucosal surfaces often grow as adherent colonies composed of a few to a score of individual organisms (*1, 2*). This colonial mode of growth is so characteristic of some species that it would seem to be an essential aspect of their pathogenicity. A particularly good example is EPEC (*3*). EPEC cause infantile diarrhea (*4*); when small bowel biopsies of infected children are performed, colonies of EPEC are found attached to the underlying epithelia, and effacement of the associated microvillae is evident (*5*). Similar findings are also seen in vitro with the use of cultured epithelial cells to which EPEC readily adhere as discrete clusters of bacteria, a phenomenon that is termed localized adherence (LA) (*6, 7, 8*). From these observations it is apparent that the bacteria within these colonies interact not only with the host cells to which they are bound but also with each other. We have identified and characterized a unique surface appendage of EPEC that seems to be associated with this colonial mode of growth.

B171, an EPEC strain of serotype 0111:NM, exhibits the LA phenotype in vitro (*9*). When B171 was propagated on colonization factor agar (CFA) (*10*) at 37°C and then examined by electron microscopy, 10 to 30 filaments were seen projecting from the surface of each bacterium (Fig. 1A). These filaments were straight, approximately 7 nm in width, and existed as well-separated, individual fibers. Their ultrastructural appearance, functional properties, and primary structure were found to be similar to the mannose-resistant *E. coli* pili described (*11, 12*). However, when B171 was grown on trypticase soy agar (TSA) supplemented with 5% defibinated sheep blood, expression of the pili was reduced, and instead, long, ropelike structures were evident (Fig. 1B). At higher magnifications these structures were seen to be composed of many laterally aggregated pilus filaments forming bundles 50 to 500 nm wide and 15 to 20 μm long. These filaments, which we call bundle-forming pili (BFP), tended to twist, curl, and form loops; moreover, bundles expressed by different organisms appeared to be intertwined, thus forming a three-dimensional meshwork, within which individual bacteria were embedded.

The production of BFP by strain B171 was influenced by temperature (optimal expression occurred at 37°C) and the composition of the growth medium. To determine if the expression of BFP could also be induced by physical and chemical variables found near the epithelial cell surface, we examined EPEC-infected HEp-2 cells by scanning electron and immunofluorescence microscopy. For these experiments, strain B171 was first grown in Luria broth, a medium that does not favor optimal expression of BFP. Then the bacteria grown in broth were inoculated into wells containing cultured HEp-2 cells and DMEM medium supplemented with 10% fetal calf serum (*13, 14*). Three hours later the LA phenomenon was evident; most epithelial cells had one to three clusters of adherent bacteria (Fig. 2A). Scanning electron micrographs of these clusters showed multiple bundles coursing between the bacteria (Fig. 2B); at the base of the colony, fibers also appeared to tether individual bacteria to the epithelial cell surface. An identical pattern was observed with EPEC strain E2348/69, serotype 0127:H6 (not shown).

To determine whether the interbacterial filaments shown in Fig. 2B corresponded to the bundled filaments depicted in Fig. 1B, we used a BFP-specific antiserum to probe these colonies for the presence of the corresponding antigen (*15*). This serum was elicited to purified BFP, refined by adsorption with strain B171 grown under conditions nonfavorable for BFP expression to remove antibodies to cell wall antigens such as lipopolysaccharide, and then shown by immunogold electron microscopy to bind only BFP (Fig. 1C), indicating that this preparation of purified BFP was largely free of the straight pili (Fig. 1A); this experiment also demonstrated that the straight pili and BFP are antigenically different. Use of this serum revealed brightly fluorescing bands within each of the bacterial clusters (Fig. 2D); this pattern of fluorescence could be readily distinguished from the pattern produced by an antiserum to *E. coli* cell-wall antigens (*12*) that stained the individual bacteria composing the cluster (Fig. 2C). Thus, we propose that BFP are expressed by EPEC growing on epithelial cell surfaces where the BFP participate in the formation of the bacterial colony by forming bundles that link one bacterium to another.

We tested this hypothesis by determining if antibodies to BFP could inhibit the LA phenomenon (*14*). Serial dilutions of the

Department of Microbiology and Immunology, Beckman Center B239, Howard Hughes Medical Institute, Stanford University, Stanford, CA 94305.

*Present address: Center for Vaccine Development, University of Maryland, 10 South Pine Street, Baltimore, MD 21201.
†To whom correspondence should be addressed.